Development and Sultan Test Result of ITER Conductor Samples of Korea

Hyoung Chan Kim, Dong Keun Oh, Soo-Hyeon Park, Keeman Kim, and P. Bruzzone

***Abstract*—As a way to improve performance of ITER TF conductors, two types of Nb_3Sn cable-in-conduit conductors were developed in Korea with variations of conduit thickness resulting in the different void fraction of the conductors. The estimated void fractions of the conductors are 31% and 33%. Here we report the details of the TF conductor development and the performance test result of them carried out in SULTAN. Regarding the conductor development, the internal-Sn-processed Nb_3Sn strand characteristics, strand cabling, twist pitch and characteristics of the conduits for the conductors are presented. For an extended understanding of the conductor design and performance, the SULTAN test results are presented and the effect of the void fraction variations is discussed based on the results.**

***Index Terms*—Cable-in-conduit conductor, Internal-Sn Nb_3Sn, ITER TF, void fraction.**

I. Introduction

FOR the development of reliably performing TF conductors of ITER magnets, series of development, test, and investigations on the TF conductors have been made in collaboration under the ITER project [1], [2]. In 2006, a few design modifications of TF conductor was suggested and based on the renewed layout, conductor samples were developed and short sample performance test were carried out by ITER participants. Based on the results of this conductor R&D program, the optimized conductor design specifications are expected to be drawn out for the ITER magnet.

The understanding of cable-in-conduit conductors is a long-lasting scientific problem since its conception in 1970's [3]. Though several types of cable-in-conduit conductors were designed and fabricated for the superconductor magnet applications in last decades, ITER magnet system led us to face an another aspect of superconducting conductors with respect to its large size and the Nb_3Sn strands used for it. Assessing and understanding the correlation between the Nb_3Sn strand characteristics and the conductor performance under electromagnetic loading, and the effects of conductor design parameters such as cabling pattern and void fraction on the conductor performance are challenging technological steps to the development of well-performing stable superconducting conductors.

Manuscript received August 27, 2007. This work was supported by the Ministry of Science and Technology of Republic of Korea under the ITER Project Contract.

H. C. Kim, D. K. Oh, S.-H. Park, and K. Kim are with the National Fusion Research Institute, Daejeon 305-333, Korea (e-mail: chankim@nfri.re.kr).

P. Bruzzone is with EPFL-CRPP, Fusion Technology, 5232-Villigen PSI, Switzerland (e-mail: pierluigi.bruzzone@psi.ch).

Color versions of one or more of the figures in this paper are available online at http://ieeexplore.ieee.org.

Digital Object Identifier 10.1109/TASC.2008.921256

As a participant taking part in the ITER TF conductor R&D program, we have developed and fabricated two TF conductors (KOTF) and the conductor performance test was carried out in SULTAN facility of CRPP. Along with the conductor specifications based on the ITER TF design in 2004 [4], we varied the conduit thickness in two ways such that two kinds of conductor samples having different void fraction were produced. With the other conductor parameters kept the same, we can expect to single out and compare the effect of different void fraction on the conductor performance. In this paper, we present the details of KOTF conductor fabrication and the test result of them carried out in SULTAN.

II. KOTF Conductor Sample Fabrication

A. Nb_3Sn Strand Characteristics

For the fabrication of KOTF conductors, we used internal-Sn-processed Nb_3Sn strands (KAT RC38c6b7A, KAT, Korea). The billet for the strand was produced by restacking the 19 Nb-Sn sub-elements with Cu and Sn spacers in Cu (OFHC) tube. The Cu stabilizer tube and the sub-elements are separated with Ta barrier. A sub-element consists of 175∼180 Nb-rods surrounding a Sn core. After twisting and final drawing, the strand was plated with 2 μm thickness Cr. The diameter of strand is 0.82 mm and twist pitch is 15 mm with right hand twist direction. After heat treatment, the filament diameter of the strand is $5.0 \sim 5.5$ μm. The critical current density J_c measured at 12 T, 4.2 K on ITER barrel is 899 A/mm^2 and n-value measured at the sample temperature and field conditions is 33. The measured J_c is consistent with I_c measurement result of the SULTAN witness strand sample which was heat treated with the same heat treatment scenario [5]. The hysteresis loss Q_h measured at 4.2 K with a ± 3 T magnetic field cycling is 772 mJ/cc and the residual resistivity ratio (RRR) of the strand is 126. The Cu/non-Cu ratio estimated by cross-sectional contour of the strands is 0.97. The specifications of the Nb_3Sn strand used for KOTF conductor is summarized in Table I and the further characterizations of the strand such as $J_c(B, T, \varepsilon)$ scaling parameterization and the cross-sectional view before and after reaction heat treatment is presented by other paper [6].

B. Conductor Cabling Specifications

The cabling patterns of KOTF conductor are those of ITER TF baseline description, $((2\,SC{+}1\,Cu){\times}3{\times}5{\times}5{+}Cu\,core){\times}6$ with 3×4 Cu core [4]. The Cu strand used for the conductor was produced by drawing from OFHC billet of 8 mm diameter. The Cu strand was Cr-plated with 2 μm thickness as the Nb_3Sn

TABLE I
Nb_3Sn STRAND SPECIFICATIONS

SC Strand	Original Conductor Design	Measurement Data (KOTF)
Diameter	0.82 ± 0.003 mm	0.82 mm
Twist pitch	15 mm	15 mm
Twist direction	Right hand	Right hand
Cr plating	2.0 ± 0.1 μm	2.0 μm
J_c (12 T, 4.2 K) on ITER barrel	> 800 A/mm^2	899 A/mm^2
Q_h (±3 T cycle, 4.2 K)	< 1000 mJ/cc non-Cu	772 mJ/cc
RRR	> 100	126
n value(12 T, 4.2 K)	> 20	33

strand. The diameter of Cu strand is 0.82 mm and the measured RRR is 438.

The 5 stage twist pitch of the conductor cabling is 41.5 ± 0.5 mm, 80 ± 1 mm, 125 ± 2 mm, 240 ± 3 mm, 450 ± 10 mm with the central core (3 × 4) twist pitch 41.5 ± 0.5 mm, 81 ± 1 mm. The cable wrapping was done using 40 mm width, 0.08 mm thickness 316 L tape with 35% overlapping in left hand direction. For the sub-cable wrap, 15 mm width, 0.05 mm thickness 316 L tape was used with 50% open surface in left hand direction. The central spiral working as central He flow channel for TF conductor is a spiral tube with 30% open surface twisted in left hand direction. The outer diameter of 316 L central spiral used for the conductor was 9 mm with 1 mm thickness.

The cabling was done using 2-roll multi-stage motor-driven roller system (Nexans Korea). Before going into Nb_3Sn strand cabling, several trial cabling using hard Cu strands had been made to find out the optimal cabling conditions. The cable undergone the 5 stage twist cabling was drawn into the jacketing tube and compacted to the final size of the cable-in-conduit conductor. The conductor diameter is 43.7 mm (±0.1 mm). The conductor cabling specifications are listed in Table II.

C. Jacketing Tube Characterization

316 LN (POSCO Specialty Steel, Korea) was employed for the conductor jacketing tube material. We prepared two jacketing tubes which differ in thickness, 1.6 mm and 1.9 mm. Beginning with the same tube outer diameter of 46.5 mm, the jacketed cable was drawn through compaction roller to the 43.7 mm diameter cable-in-conduit conductor. The effective He flow region between the central spiral and the conduit inner wall varies according to the void fraction of the conductors. The estimated void fractions are 33% for 1.6 mm thickness conduit conductor and 31% for 1.9 mm thickness conduit conductor. As one of the main design parameters for assessing the performance of a cable-in-conduit conductor is void fraction of the conductor, it is the primary objective of this study to test and investigate the effect of different void fraction on the conductor performance. The test results will be discussed in detail in later sections. Fig. 1 shows the cross-sectional view of the two KOTF conductors.

Due to the large electromagnetic force exerted on the TF conductor in operation, mechanical strength at cryogenic temperature is an immediate concern on the jacket material. We measured mechanical strength of the jacket material employing standard tensile test method at room temperature (ASTM A370) and at 4.2 K (ASTM E1450). The test specimens were cut from the conduit used for conductor production by electric discharge wire cutting. For the test at cryogenic temperature, the tensile test machine (MTS Alliance RT/100) was equipped with liquid He cryostat.

Fig. 2 shows tensile test result of two conduit samples measured at 4.2 K. The heat treatment was done according to the same heat treatment scenario as was done for Nb_3Sn strand. After compaction, both the yield strength and the tensile strength increase significantly due to the work hardening effect introduced by the compaction. On the other hand, the heat treatment decreases the strengths slightly that can be attributed to the growth of grain size of the material. The fraction of the yield strength decrease due to heat treatment in the 1.9 mm thickness compacted tube sample shown in Fig. 2 is about 4.3%. In Table III, tensile test results of four conduit samples measured at room temperature and 4.2 K are summarized. All of the yield strength at 4.2 K are larger than 950 MPa requirement [7]. Another notable thing of the results is the quite

TABLE II
CONDUCTOR CABLING SPECIFICATIONS

Jacketed Conductor	KOTF(L)	KOTF(R)
Cabling patterns	((2SC+1Cu))×3×5×5 + central core)×6 Central core: Cu 3×4	
Twist pitch (mm)	41.5±0.5 mm, 80±1 mm, 125±2 mm, 240±3 mm, 450±10 mm Central core: 41.5±0.5 mm, 81±1 mm	
Cable wrap	40 mm × 0.08 mm, 35% overlapped, left hand, 316L	
Sub-cable wrap	15 mm × 0.05 mm, 50% open surface, left hand, 316L	
Central spiral	ID 7 mm × OD 9 mm, 30% open surface, left hand, 316L	
Jacket material	316LN	
Conductor diameter	43.7 mm (±0.1 mm)	
Jacket thickness & inside diameter	1.6 mm, 40.5 mm (±0.1 mm)	1.9 mm, 39.9 mm (±0.1 mm)
Void fraction (estimation)	33%	31%

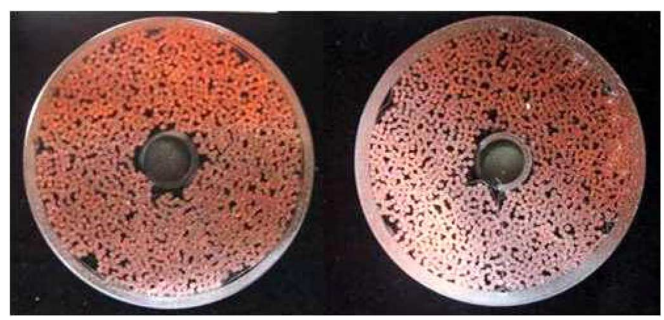

Fig. 1. Cross sectional view of the two KOTF conductors. The estimated void fraction and the conduit tube thickness of the left leg are 33%, 1.6 mm and those of the right leg are 31%, 1.9 mm.

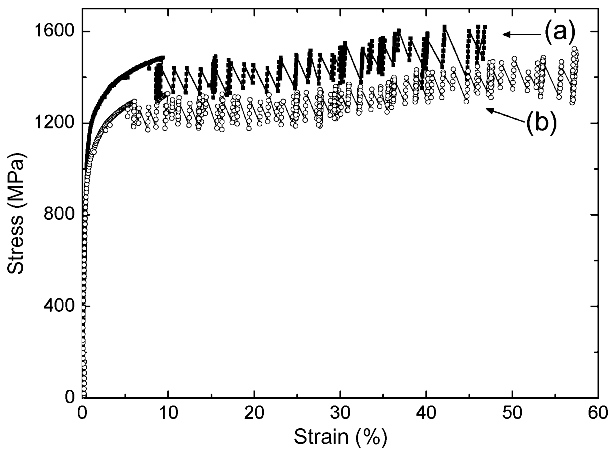

Fig. 2. Tensile test result of KOTF conduit specimens measured at 4.2 K. From top to bottom, (a) compacted and heat treated, 1.9 mm thickness, (b) uncompacted and heat treated, 1.6 mm thickness.

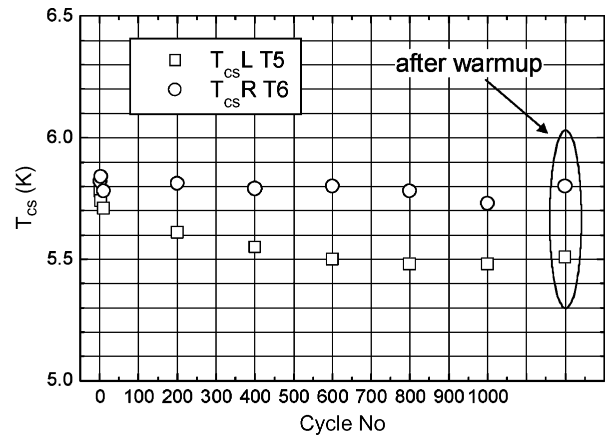

Fig. 3. T_{cs} evaluation results at several stages between cyclic loads. The left leg (TcsLT5) is 33% void fraction sample and right leg (TcsRT6) is 31% void fraction sample.

TABLE III
MECHANICAL STRENGTH OF THE CONDUIT MATERIALS MEASURED AT ROOM TEMPERATURE AND 4.2 K

Specimen	Thickness (mm)	Y. S. (MPa)	T. S. (MPa)	Elongation (%)
At Room Temperature				
Compacted	1.6	550	730	38.8
	1.9	570	761	43.6
Compacted & Heat Treated	1.6	470	727	41
	1.9	480	746	43.2
At 4.2 K				
Compacted	1.6	1160	1650	38
	1.9	1170	1663	51
Compacted & Heat Treated	1.6	1050	1594	42
	1.9	1120	1620	42

large elongation ranging from 38% up to 51% at 4.2 K, which is much larger than the 30% requirement.

D. Heat Treatment

The heat treatment schedule employed for KOTF conductor was: 210 °C for 50 hours, 340 °C for 25 hours, 450 °C for 25 hours, 575 °C for 100 hours, 650 °C for 100 hours, and then natural cooling to room temperature. The temperature ramp rate was kept to 5°C/h. The heat treatment of Nb_3Sn strands and jacketing tube samples used for the characterization was carried out in tube furnace in vacuum following the same schedule. With 100 hours duration at 650 °C, we expected some enhancement of Nb_3Sn strand stability by preventing excessive Cr diffusion into the inside of the strand.

III. SULTAN TEST RESULTS

As the SULTAN test of the conductor R&D program was intended to assess the effect of the conductor configuration such as void fraction and cabling pattern on the conductor performance, the test aimed at the evaluation of current sharing temperature T_{cs} under repeated electromagnetic loading up to 1000 cycles. T_{cs} measurement was done at 68 kA current under 10.78 T external field with the central channel blocked enforcing He flow into the cable. The conductor sample of lower void fraction (estimated value 31%) was installed as right leg (KOTF_R) and the conductor sample of the estimated 33% void fraction was installed as left leg (KOTF_L). The voltage taps and temperature sensors are attached to the outer surface of conductor jacketing tube. Since a significant transient voltage is generated during temperature increase, the conductor temperature was measured after temperature stabilization with stepwise temperature increase. The details of SULTAN sample preparation and measurement methodology are given in [5] and the references therein.

Fig. 3 shows the result of T_{cs} evolution with cyclic loading. Because the negative voltage drift observed in KOTF_L during current ramp is not a measure of the longitudinal electric field needed for T_{cs} assessment, T_{cs} of KOTF_L was determined after subtracting the offset voltage. The accuracy of the T_{cs} assessment is estimated to be better than ±0.1 K [5]. Initial T_{cs} of the samples with different void fraction were not so much different and both of them were above 5.7 K. However T_{cs} evolution with cycling load showed different behavior for the two samples. While KOTF_L showed a discernible degradation behavior with cycling load and a converging behavior around 5.5 K after 600 cycles, KOTF_R showed almost non-degrading T_{cs} behavior up to 1000 cycles. T_{cs} of KOTF_R remained above 5.7 K when it was re-cooled down after 1000 cycles. From the result, we can see that more compactly cabled conductor by lowering the void fraction are more robust against electromagnetic force acting on the cable.

Fig. 4 shows calorimetric T_{cs} evaluation of KOTF_R by steady state He flow method. T6 and T8 are temperature sensors attached on the opposite side of KOTF_R, 250 mm upstream to the high field center. Because temperature readings of the two sensors were quite different due to the complications caused by non-uniform current and He distribution, we cannot determine T_{cs} directly from the result. However we can see clearly the non-degrading behavior of KOTF_R with

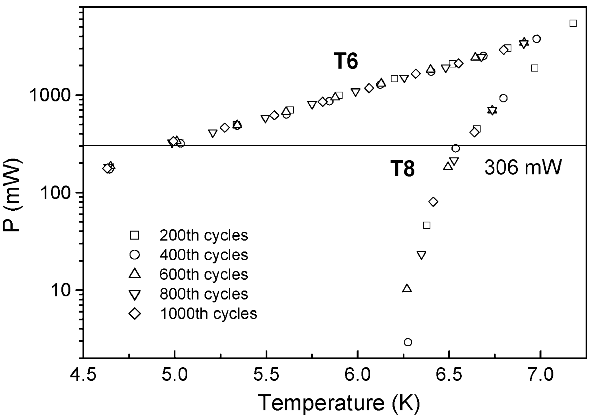

Fig. 4. The steady state He flow calorimetric measurement result of KOTF_R under cyclic loading. The horizontal line is for power dissipation equivalent to 10 μV/m current sharing electric field.

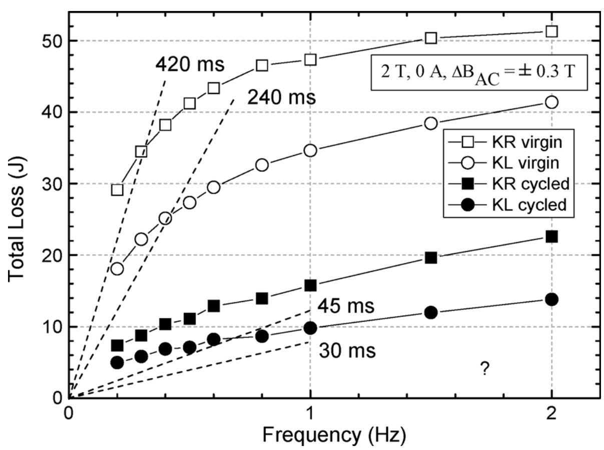

Fig. 5. AC loss measurement result of KOTF samples before and after cycling load. DC background field was 2 T and ± 0.3 T alternating field was applied for the measurement.

respect to cyclic loading. The temperature corresponding to the power dissipation equivalent to current sharing electric field $(306 \text{ mW} \equiv 10\ \mu\text{V/m})$ remained almost unchanged up to 1000 cycles.

AC loss of the two conductor samples measured before and after cycling load are shown in Fig. 5. The AC loss of KOTF_R was larger than that of KOTF_L and AC loss of both of the sample became considerably smaller after cyclic loading. The larger AC loss of a sample with lower void fraction can be explained by the increased inter-strand coupling loss. The noticeably reduced AC loss after cyclic loading implies that the friction inside the strand bundle under AC field became decreased after cyclic loading. Because of the quite large Lorentz force acting on the strands in SULTAN test condition, the strand bundle tends to be compacted to the direction of Lorentz force under cyclic loading. The AC loss result supports the DC measurement result in that more compacted cable shows more rigidity against applied electromagnetic load.

IV. Discussion

As was addressed in the Introduction section, one of the features of two KOTF samples that we give attention to is the different void fraction of the conductors. Considering that lots of studies on TF conductor performance have been focused on the constituting strand characterization and the correlation between them, the test results of this study point out the role of conductor design factors such as void fraction and twist pitch. Reflecting the test result of TFPRO2 of EU that showed an outstanding conductor performance with longer initial twist pitch [8], we can see that more compacted cable by lower void fraction and not-excessively twisted strand cable provide a conductor with the condition that renders lessened strain and breakage of Nb_3Sn strands under electromagnetic force.

Another aspect of the different behavior of the two KOTF conductor samples is the transient voltage response during stepwise temperature increase at the temperatures above T_{cs}. More pronounced transient voltage generation is observed in the conductor sample of lower void fraction when He inlet temperature was stepwise increased above T_{cs} (not shown here). Because significant current sharing exists in the conductor above T_{cs}, the pronounced transient voltage response signifies the stability of the conductor became marginal. Since this behavior can be caused by the reduced He flow channel of the conductor sample, lower void fraction provides two contrasting effects on the stability with respect to cycling electromagnetic load and thermo-hydraulics. Considering the central spiral He channel that will work in actual TF magnet operation, we can expect the reduced He flow channel in the cable region with lower void fraction is compensated by working central spiral.

V. Conclusion

We described about the details of KOTF conductors. On the conductor fabrication side, internal-Sn processed Nb_3Sn strand development and characterizations, strand cabling specifications, characterizations of jacketing tube, and reaction heat treatment specifications were presented. The SULTAN test results of the two conductor samples suggest that optimizing the conductor configuration such as void fraction is effective on the conductor performance under cycling load. The conductor with lower void fraction showed stable performance in the test condition while the conductor with larger void fraction was more susceptible to repeated electromagnetic load resulting in discernible performance degradation.

References

[1] N. Mitchell, “Summary, assessment and implications of the ITER model coil test results,” *Fusion Engineering and Design*, vol. 66–68, pp. 971–993, 2003.

[2] P. Bruzzone *et al.*, “Test results of two ITER TF conductor short samples using high current density Nb3Sn strands,” *IEEE Appl. Supercond.*, vol. 17, 2007, to appear.

[3] L. Dresner, “Twenty years of cable-in-conduit conductors: 1975–1995,” *Journal of Fusion Energy*, vol. 14, no. 1, pp. 3–12, 1995.

[4] ITER Final Design Report Jan. 2004, ITER IT Design Description Document, unpublished.

[5] P. Bruzzone *et al.*, “Results of a new generation of ITER TF conductor samples in SULTAN,” presented at the MT20 Conference, paper 2D01.

[6] S. Oh *et al.*, “A variable temperature Walter spiral probe for the critical current measurement of superconducting strands,” presented at the MT20 Conference, paper 3J08.

[7] Specification and Performance Database for Steel Jackets for Nb_3Sn Conductors, ITER Design Description Document, Jul. 2005.

[8] P. Bruzzone *et al.*, “Test results of two European ITER TF conductor samples in SULTAN,” presented at the MT20 Conference, paper 4I06.